Afyon Kocatepe Üniversitesi Fen ve Mühendislik Bilimleri Dergisi

Afyon Kocatepe University Journal of Science and Engineering

AKÜ FEMÜBİD **18** (2018) 011106(90- 102) AKU J. Sci. Eng. **18** (2018) 011106 (90-102)

DOİ: 10.5578/fmbd.66546

Experimental and Theoretical Studies on Theobromine and Theobromine-Water Complexes

Mustafa Tuğfan BİLKAN

Department of Physics, Faculty of Science, Çankırı Karatekin University, 18100 Çankırı, Turkey
e-posta: mtbilkan@gmail.com

Geliş Tarihi:16.05.2017 ; Kabul Tarihi:10.04.2018

Keywords
Theobromine; Solvent effects; Hydrogen bonds; Vibrational spectroscopy; Density Functional Theory

Abstract

In this study, the solvent effects on structural, spectroscopic, electronic and thermochemical properties of Theobromine (tbH) were theoretically investigated. The dichloromethane (DCM), dimethylsulfoxide (DMSO) and water (H_2O) solvents have been chosen for investigations. Optimized molecular structures of tbH were obtained by using the DFT/B3LYP method with 6-311++G(d,p) basis set in vacuum and in solvent media. Calculated geometric structure parameters were compared with experimental data. In the experimental section, the mid-IR spectrum of tbH was recorded using ATR equipment and compared with calculated vibrational frequencies. tbH-H_2O complexes were studied for various binding ratios. The total energies and hydrogen bond lengths of these complexes were discussed in detail. It is seen as the result of this study that N···H-O and O···H-O non-covalent bonded structures are more stable for all binding versions and hydrogen bond lengths for all tbH-H_2O complexes range from 1.8-2.5 Å.

Teobromin ve Teobromin-Su Bileşikleri Üzerine Deneysel ve Teorik Çalışmalar

Anahtar kelimeler
Teobromin; Çözücü etkileri; Hidrojen bağları; Titreşim spektroskopisi; Yoğunluk Fonksiyonel Teorisi

Özet

Bu çalışmada Teobromin'in (tbH) yapısal, spektroskopik, elektronik ve termokimyasal özellikleri üzerine çözücü etkileri teorik olarak incelenmiştir. İncelemelerde, diklorometan (DCM),dimetilsülfoksit (DMSO) ve su (H_2O) çözücüleri seçilmiştir. tbH'nin optimize edilmiş moleküler yapıları, DFT/B3LYP metodu ve 6-311++G(d,p) temel seti kullanılarak vakum ve çözücü ortamlarda elde edilmiştir. Çalışmanın deneysel kısmında, tbH orta-bölge IR spektrumu, ATR sistemi ile kaydedilmiş ve deneysel sonuçlar hesaplanan verilerle kıyaslanmıştır. Farklı bağlanma oranları için, tbH-H_2O bileşikleri çalışılmıştır. Bileşiklerin toplam enerjileri ve hidrojen bağ uzunlukları detaylı bir şekilde incelenmiştir. Yapılan bu çalışmanın sonuçlarından N···H-O ve O···H-O tipi kovalent bağlı olmayan yapılar, diğer tüm bağlanma durumlarından daha kararlıdır ve bileşiklerin hidrojen bağ uzunlukları 1.8-2.5 Å aralığında değişmektedir

1. Introduction

Ligand-water interaction is an important issue in the search for bio-molecular activities because most living organisms contain water and all biological processes occur in the aquatic environment in living cells. Generally, such interactions occur in the form of hydrogen-bonded compounds. In these compounds, a water molecule is often bound to the ligand molecules or other water molecule by a hydrogen bond. For example, nucleobases interact via hydrogen bonds (Fornaro *et al.* 2015). Due to its importance, there are many published studies in the literature in this topic (Parthasarathi *et al.* 2005, Calabrese *et al.* 2016, Kwak *et al.* 2008, Bernar *et al.* 2009). In calculating physical and chemical properties of any molecular system, hydrogen-bonded interactions are important, but they have some burdensome aspects. Although the determination of a potential energy surface for biomolecule-water complex systems, using ab initio techniques, is extremely difficult, these techniques

can provide valuable insight into the details of the interaction (Mourik *et al.* 1999). Also, ab initio techniques can provides important facilities to study of the physical and chemical properties of complex systems with inter and intramolecular interactions.

In this paper, solvent effects on spectroscopic and structural properties of theobromine (tbH) were studied in detail. tbH is an important alkaloid. It has been investigated by scientists for many years because of its commercial and scientific importance (Cook and Regnier 1967, Mikulski *et al*. 2007, Ford *et al*. 1998). It is also known with biological and pharmacological activities in living organisms (Oettle and Reibnegger 1999, Tewari *et al.* 2012). To the best of our knowledge, there are not enough studies in the literature on the investigation of solvent effects on tbH. Recently, we published a solvent effect study on tbH (Bilkan 2017). In the past, Ucun et al. have done some quantum chemical calculations on molecular structures and vibrational frequencies of various xanthine derivatives by Hartree-Fock and Density Functional Theories (Ucun *et al*. 2007). In this study, for the investigation of solvent effects on tbH, basically two strategies were used, including implicit and explicit. The solvent effects were investigated in different solvent media (polar protic, polar aprotic and nonpolar) using the Polarizable Continuum Model (PCM) (Miertus *et al*. 1981). Subsequently, the tbH-H_2O complexes were examined for different binding ratios. The solid-phase experimental FT-IR spectrum of tbH was recorded and compared with the calculated vibrational data. Moreover, some important electronic properties such as the electrophilicity (ω), global hardness (η), chemical potential (μ), ionization potential (I) and electron affinity (A) (Wang *et al.* 2015) were calculated to identify the nature of pharmacological properties of tbH.

2. Materials and Methods

2.1. Computational methods

The energies, thermochemical properties, optimized molecular structures, vibrational frequencies and electronic properties of tbH were calculated using the Gaussian03 program and the Gaussview visualization program (Frisch *et al.* 2003, Denington *et al.* 2008). The calculated frequencies were scaled by 0.9668 (Yurdakul and Bilkan 2015) to correct for the difference between the calculated and the experimental vibrational frequencies. Firstly, the optimized molecular structures of tbH in vacuum and solvent media were performed using by 6-311++G(d,p) basis set. Secondly, based on the optimized structures, some of physical and chemical properties were calculated. The fundamental vibrational modes were characterized by their PED (potential energy distribution) obtained by using the VEDA4 program (Jamróz 2004).

2.2. Experimental procedures

In the experimental section of this study, tbH was purchased from Sigma-Aldrich and used without further purification. The infrared spectrum of tbH was recorded between 3700-550 cm^{-1} by PerkinElmer 100 spectrum FT-IR spectrometer with Attenuated total reflection (ATR) equipment in Çankırı Karatekin University Central Research Laboratory.

3. Results and Discussions

3.1. Molecular structure and geometry optimization

The optimized molecular structure of tbH is present in Figure 1. The bond lengths and bond angles of optimized structures are given in Table 1. The selected experimental values of molecular parameters were taken from the literature 9 and compared with the calculated ones in Table 1.

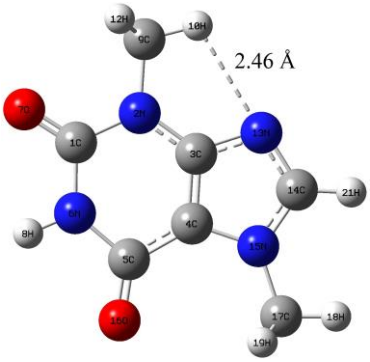

Figure 1. Optimized molecular structure of isolated tbH

Solvent effects on the geometry of tbH were investigated using three different solvents. As can be seen from Table 1, in most cases, calculated bond

lengths are in good agreement with the experimental data. The calculated bond lengths have minor deviations compared to the experimental ones. Moreover, there are minor variations in bond length values calculated in different solvent environments.

Table 1. Optimized geometric parameters of tbH in different solvent media.

Lengths	Vacuum	Non-polar	Polar		Exp.*
		DCM	DMSO	H_2O	
1C-2N	1.393	1.386	1.385	1.385	1.377
1C-7O	1.215	1.222	1.223	1.223	1.231
3C-4C	1.383	1.385	1.386	1.386	1.364
3C-13N	1.371	1.370	1.370	1.370	1.363
4C-5C	1.434	1.430	1.429	1.429	1.426
4C-15N	1.403	1.403	1.403	1.403	1.388
5C-6N	1.411	1.407	1.407	1.407	1.397
5C-16O	1.220	1.225	1.226	1.226	1.225
6N-8H	1.012	1.013	1.013	1.013	0.856
14C-15N	1.343	1.339	1.339	1.339	1.343
14C-13N	1.292	1.296	1.296	1.296	1.339
2N-9C	1.465	1.467	1.467	1.467	1.473
9C-10H	1.087	1.086	1.086	1.086	1.039
9C-12H	1.092	1.090	1.090	1.090	0.971
17C-20H	1.090	1.089	1.089	1.089	1.034
Angles					
2N-1C-6N	115.34	115.74	115.79	115.79	116.37
2N-1C-7O	122.68	122.57	122.57	122.57	122.10
6N-1C-7O	121.99	121.70	121.64	121.64	121.53
4C-3C-13N	110.77	110.80	110.80	110.80	112.72
4C-3C-2N	122.86	122.89	122.89	122.89	122.40
3C-4C-5C	122.84	122.44	122.39	122.39	122.94
4C-5C-16O	128.58	128.71	128.74	128.74	128.63
15N-14C-13N	116.50	116.75	116.78	116.78	114.30
4C-15N-14C	103.93	103.88	103.87	103.87	105.62
1C-2N-3C	119.23	119.11	119.09	119.09	118.91
3C-2N-9C	122.04	122.12	122.11	122.11	121.76
1C-6N-5C	130.05	129.77	129.72	129.72	129.10
1C-6N-8H	114.16	114.40	114.43	114.43	116.67

*Data were taken from Ref [Ford et al..

The calculated C-C and C-N bond lengths are very close to the experimental values. Deviations between calculated and experimental values are less than 0.02 Å. Importantly, since the bond between atoms 3C-4C is a double bond, the bond length of 3C-4C atoms is shorter than the bond length of 4C-5C atoms. Compatibility with the experiment was also observed in the calculation of C-O bond lengths. Both 1C-7O and 5C-16O bond lengths were calculated in accordance with the experimental data. When Table 1 is analyzed, it is evident that the 6N-8H bond length is calculated as 1.012 Å in vacuum and 1.013 Å in the solvent media, but experimental value is 0.856 Å. Similarly, C-H bond lengths are an average of 1.080-1.090 Å for the structure while experimental values are between of 0.891-1.064 Å. The reason of these deviations is low scattering factors of hydrogen atoms in X-ray diffraction.

Figure 1 shows an intramolecular hydrogen bond between nitrogen and hydrogen atoms for tbH. The distance between the 13N and 10H atoms is 2.46 Å. It is well known that this distance between the nitrogen and hydrogen atoms indicates the intramolecular hydrogen bonding (Brandle *et al*. 2001). Since the distance between 7O-12H is 2.75 Å and the distance between 8H-16O is 2.99 Å, we do not think that there are intramolecular hydrogen bonds between the atoms. As with bond lengths, the solvent medium also affects the bond angles, but most of the angles are consistent with the experimental values. In addition, Table 1 shows that the geometric parameters calculated in the polar and non-polar solvent environments are different from each other. This indicates that different polarities lead to the formation of different geometric structures.

3.2. Vibrational frequencies and assignment

tbH has 21 atoms and 57 vibrational modes. All of the calculated frequencies and intensities are given in Table 2 together with experimental data. Theoretical calculations were carried out under the harmonic approximation by using B3LYP level with 6-311++G(d,p) basis set. The experimental IR spectrum of tbH in solid phase is also presented in Figure 2.

Table 2. Vibrational frequencies and assignments of tbH in different media.

Mode	Exp.	Vacuum		DCM		DMSO		H_2O		(%) PED
		Freq.	IR	Freq.	I_{IR}	Freq.	I_{IR}	Freq.	I_{IR}	
1	-	28	0.00	42	0.00	35	0.00	33	0.00	$\Gamma_{HCNC}(74)+\Gamma_{CCCN}(13)$
2	-	55	0.13	67	0.20	73	0.21	74	0.21	$\Gamma_{HCNC}(41)+\Gamma_{CCCN}(39)$
3	-	91	0.01	94	0.02	94	0.03	94	0.03	$\Gamma_{NCNC}(54)+\Gamma_{CNCC}(11)$
4	-	107	0.21	112	0.12	113	0.12	113	0.12	$\Gamma_{CCCN}(36)+\Gamma_{NCNC}(24)$
5	-	138	0.61	146	0.45	146	0.44	146	0.44	$\Gamma_{NCNC}(44)+\Gamma_{CNCC}(30)$
6	-	186	0.32	193	0.26	194	0.26	194	0.26	$\Gamma_{CCCN}(41)+\Gamma_{NCNC}(36)$
7	-	204	1.29	203	1.08	204	1.04	204	1.04	$\delta_{CNC}(34)+\delta_{NCN}(28)$
8	-	218	0.22	224	0.19	225	0.20	225	0.20	$\Gamma_{CCCN}(52)+\Gamma_{CNCN}(13)$
9	-	296	0.20	295	0.19	296	0.19	296	0.19	$\delta_{CNC}(69)$
10	-	341	0.01	346	0.00	347	0.00	348	0.00	$\Gamma_{CNCN}(35)+\Gamma_{NCNC}(30)$
11	-	360	1.58	360	1.46	359	1.49	359	1.49	$\delta_{OCN}(35)+\delta_{CNC}(33)$
12	-	388	0.37	387	0.24	387	0.26	387	0.26	$\delta_{OCN}(31)+\delta_{CNC}(17)+V_{CN}(11)$
13	-	432	2.80	434	2.31	434	2.31	434	2.31	$\delta_{CNC}(34)+\delta_{NCN}(14)+V_{CN}(11)$
14	-	493	1.87	498	1.61	497	1.60	497	1.60	$\delta_{CNC}(16)+\delta_{NCN}(12)$
15	555vw	584	0.88	586	0.73	585	1.29	585	1.40	$V_{CN}(66)$
16	572vw	589	0.00	587	0.50	586	0.74	586	0.74	$\Gamma_{CNCN}(50)+\Gamma_{HNCC}(16)$
17	614s	611	8.85	602	6.84	599	6.33	599	6.25	$\Gamma_{HNCC}(70)+\Gamma_{CNCN}(18)$
18	-	658	0.81	660	0.66	660	0.67	660	0.68	$\delta_{NCN}(34)+V_{CN}(21)$
19	681s	689	1.38	687	0.89	686	0.88	686	0.88	$\Gamma_{ONCC}(35)+\Gamma_{NCNC}(25)+\Gamma_{CCNC}(20)$
20	731s	709	1.45	709	1.44	709	1.44	709	1.44	$\delta_{OCN}(53)+\delta_{NCN}(13)$
21	750s	726	4.79	726	3.33	726	3.30	726	3.30	$\Gamma_{ONNC}(66)$
22	762m	734	0.14	735	0.22	735	0.25	735	0.26	$\Gamma_{ONCC}(47)+\Gamma_{ONNC}(23)+\Gamma_{CCNC}(19)$
23	783m	757	0.76	756	0.35	755	0.32	755	0.32	$V_{CN}(32)+\delta_{CNC}(16)$
24	860s	813	1.40	833	0.87	837	0.85	837	0.84	$\Gamma_{HCNC}(85)+\Gamma_{CNCN}(12)$
25	940vw	914	0.80	916	0.67	916	0.66	916	0.66	$\delta_{CNC}(25)+V_{CN}(13)$
26	-	1015	0.36	1017	0.74	1017	0.82	1017	0.83	$V_{CN}(21)+\delta_{CNC}(18)$
27	1041w	1045	2.02	1047	1.81	1047	1.85	1047	1.86	$\Gamma_{HCNC}(38)+V_{CN}(17)+\delta_{NCN}(15)$
28	1071w	1094	7.45	1097	7.12	1097	7.27	1097	7.28	$V_{CN}(48)+\delta_{CCN}(10)$
29	-	1110	0.00	1110	0.00	1109	0.01	1109	0.01	$\Gamma_{HCNC}(69)+\delta_{HCH}(30)$
30	-	1113	0.21	1110	0.01	1110	0.00	1110	0.00	$\Gamma_{HCNC}(61)+\delta_{HCH}(20)$
31	1140w	1139	0.68	1137	0.63	1138	0.73	1138	0.74	$V_{CN}(35)+\Gamma_{HCNC}(12)$
32	1173m	1185	1.66	1189	2.02	1187	2.12	1187	2.12	$\delta_{HCN}(30)+V_{CN}(10)$
33	1222s	1211	10.52	1212	10.58	1211	10.67	1211	10.68	$\delta_{HCN}(30)+V_{CN}(15)+\delta_{NCN}(10)$
34	-	1256	4.01	1261	3.79	1262	3.86	1262	3.87	$V_{CN}(40)+\delta_{CNC}(20)$
35	1293m	1296	3.64	1295	1.83	1294	1.77	1294	1.77	$V_{CN}(38)$
36	1334m	1334	6.28	1335	6.88	1335	7.37	1335	7.43	$V_{CN}(32)+\delta_{NCN}(14)$
37	1366m	1359	3.06	1361	4.14	1360	4.34	1360	4.35	$\delta_{HNC}(46)$
38	-	1370	2.04	1369	0.25	1369	0.12	1369	0.11	$V_{CN}(20)+\delta_{HNC}(13)$
39	1410m	1402	5.92	1399	6.56	1398	6.54	1398	6.53	$\delta_{HCH}(47)+V_{CN}(11)$
40	-	1409	1.00	1406	0.23	1405	0.21	1405	0.21	$\delta_{HCH}(39)$
41	1423m	1429	1.29	1425	0.99	1423	0.99	1423	0.99	$\delta_{HCH}(72)+\Gamma_{HCNC}(20)$
42	1454s	1436	16.24	1431	0.86	1429	0.88	1429	0.89	$\delta_{HCH}(44)$
43	-	1440	2.96	1432	10.80	1430	10.31	1430	10.27	$\delta_{HCH}(62)+\Gamma_{HCNC}(13)$
44	-	1462	1.93	1453	4.86	1451	4.99	1451	4.99	$\delta_{HCH}(63)+\Gamma_{HCNC}(10)$
45	1487m	1474	2.77	1470	3.66	1470	4.08	1470	4.13	$\delta_{HCH}(46)+V_{CN}(16)$

Table 2 (continuation). Vibrational frequencies and assignments of tbH in different media

46	1546s	1521	14.69	1518	11.84	1517	12.21	1517	12.26	$\delta_{CCN}(30)+V_{C\text{-}C}(19)+V_{CN}(13)$
47	1591s	1557	15.48	1550	12.40	1548	12.41	1548	12.42	$V_{C=C}(49)+V_{CN}(23)$
48	1661vs	1695	100.00	1643	100.00	1633	100.00	1632	100.00	$V_{CO}(63)$
49	1687vs	1706	78.75	1664	62.87	1656	64.68	1655	64.87	$V_{CO}(72)$
50	-	2952	3.90	2960	2.60	2960	2.53	2960	2.53	$V_{CH3Sy}(99)$
51	-	2958	2.79	2963	1.60	2964	1.55	2964	1.54	$V_{CH3Sy}(100)$
52	-	3020	1.27	3022	1.06	3022	1.08	3022	1.08	$V_{CH3ASy}(99)$
53	3014m	3027	0.63	3034	0.54	3035	0.57	3035	0.58	$V_{CH3ASy}(99)$
54	-	3040	0.75	3051	0.43	3052	0.41	3052	0.41	$V_{CH3ASy}(100)$
55	-	3062	0.04	3069	0.03	3070	0.04	3071	0.04	$V_{CH3ASy}(98)$
56	3113 w	3137	0.23	3144	0.21	3145	0.20	3145	0.20	$V_{CH}(99)$
57	3150w	3482	9.46	3475	6.94	3474	6.80	3474	6.79	$V_{NH}(100)$

vs: very strong; s: strong; m: medium; w: weak; vw; very weak, *V: stretching mode, δ: bending mode, Γ: torsional mode*

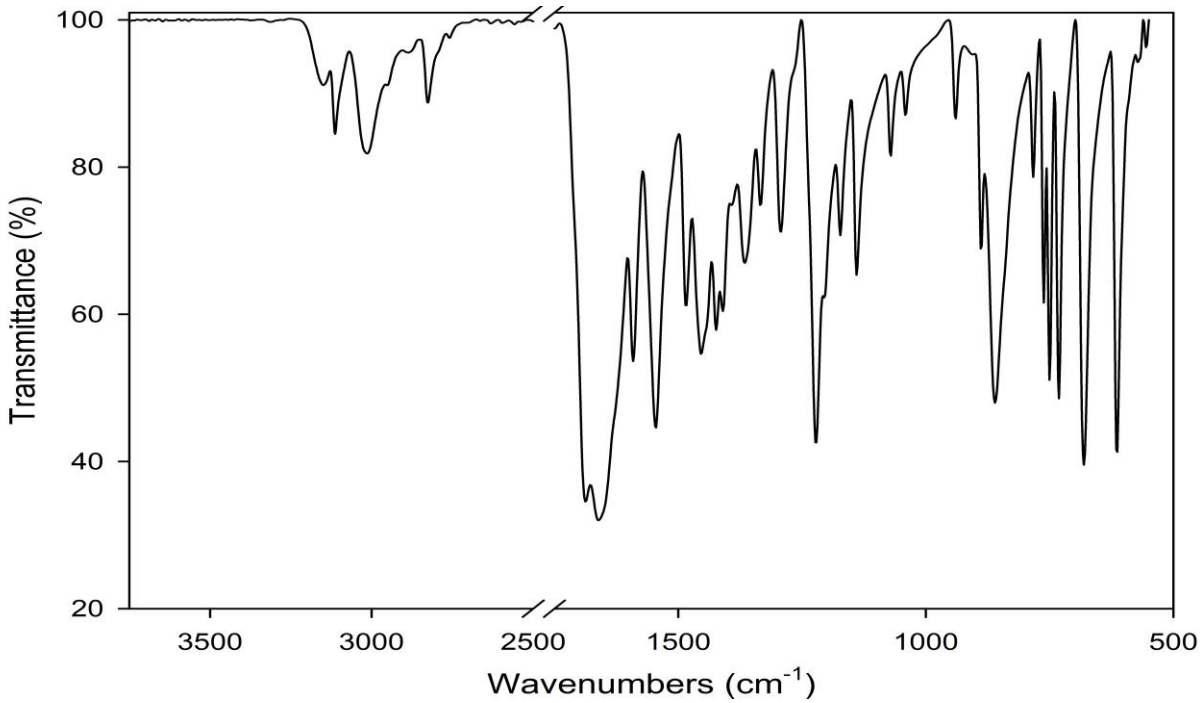

Figure 2. Experimental IR spectrum of tbH.

Small changes due to solvent effects in geometric parameters cause more serious effects on vibrational frequencies. When the effects of solvent environments on the vibrational frequency of any molecule are examined, some changes are expected. These changes are primarily shifts in the vibration frequencies due to solvent effects. Secondly, the increase or decrease in the intensity of vibration frequencies occurs. In Figures 3 and 4, these situations are evident. With increased ε, shifts in frequencies have occurred and the intensities of the vibration frequencies have increased significantly. The calculated IR spectra of tbH are also simulated in Figure 3 and Figure 4.

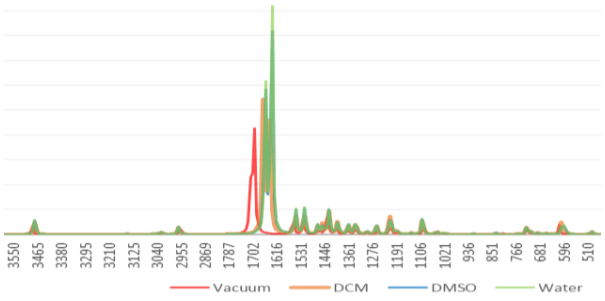

Figure 3. The comparison of theoretical IR spectra of tbH in various media.

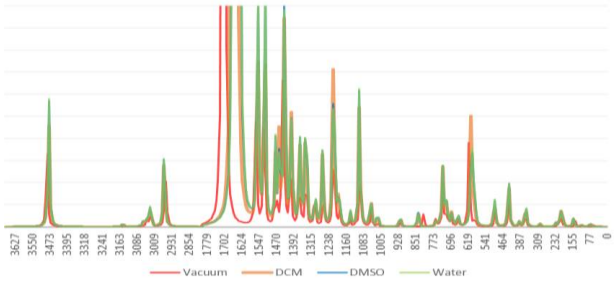

Figure 4. The comparison of theoretical IR spectra of tbH in various media (at close scale).

N-H stretching modes are seen at 3300-3500 cm^{-1} for free N-H bond. If N-H is bonded with the hydrogen bond, this value is decreased until 3100-3200 cm^{-1}. In this study, the calculated N-H stretching modes are seen at 3482 (Ɛ=1.00), 3475 (Ɛ=8.93), 3474 (Ɛ=46.83) and 3474 (Ɛ=78.36) cm^{-1} as medium intensities, but this mode is seen in the solid phase experimental spectrum at 3150w. In this case, it can be said that tbH has a bonded N-H stretching mode and therefore it may be dimeric structure in solid phase. The C-H stretching bands are found at 2900-3200 cm^{-1} region. The all of C-H stretching mode of tbH have been observed at 3113 cm^{-1} as weak in the experimental spectrum. These modes were calculated at 3137, 3144, 3145 and 3145 cm^{-1}, respectively, in vacuum and in solvent media. At the same time, tbH contains two methyl groups. The symmetric and asymmetric CH_3 stretching modes of the methyl groups are detailed in Table 2. Additionally, C=O vibrations give important information about the structure of tbH. C=O stretching modes of this structure are calculated at 1706 and 1695 cm^{-1} for vacuum while experimental values are 1691vs and 1667vs. In the DCM non-polar solvent, these modes are calculated at 1664 and 1643 cm^{-1} respectively. In the polar solvents, values of the vibrations are at 1656-1633 and 1655-1632 cm^{-1}. As can be seen from these results, the solvents affect C=O stretching vibrations of tbH too much. On the other hand, there is a difference of 26 cm^{-1} between the C=O stretching vibrations as seen from the solid tbH experimental spectrum. However, the difference between the calculated C=O stretching vibrations of free tbH is only 11 cm^{-1}. The reason of this difference is status of C=O bonds of tbH which are different from each other. In summary, we think that solid tbH is in dimeric structure and one of the C=O bond of tbH may be establish a hydrogen bond to other tbH.

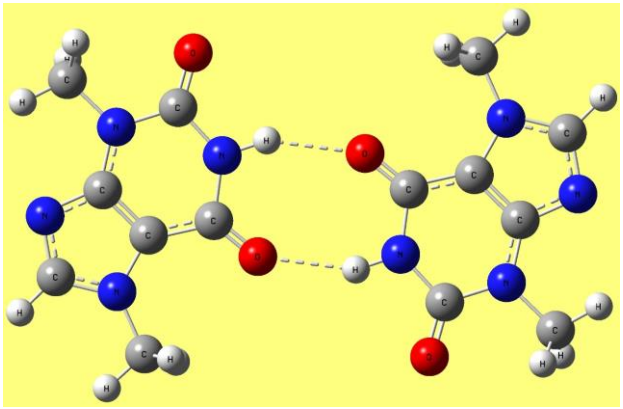

Figure 5. The possible dimer structure of tbH.

In pyrimidine rings, C-N and C-C vibration modes are seen at 1500-1600 cm^{-1} region (Breda *et al.* 2006). In this study C-C, C=C and C-N vibrational modes are calculated at 1557, 1521 and 1474 cm^{-1} in vacuum. These frequencies and their intensities are shifted seriously in solvent media. For example, in DCM medium, C=C stretching mode is calculated at 1550 cm^{-1}. In the other media, it is calculated at 1548 cm^{-1}. Furthermore, it can be seen that C=C stretching mode is more affected by the changing solvent media compared to C-C mode. Other calculated C-N stretching modes are calculated at 1334, 1296, 1256, 1139, 1094, 1015 and 757 cm^{-1}.

The bending vibrations are generally found at lower wavenumbers compared to stretching modes. H-C-N and H-N-C modes are seen in about 1200-1300 cm^{-1} region in experimental spectrum. These modes were calculated at 1359, 1211 and 1185 cm^{-1} in vacuum. Similarly, in these modes, frequency shifts are seen in the transition from gas phase to the solvent phase. The bending modes of C-N-C and N-C-N were calculated at 1045, 1015, 757, 493, 432 and 388 cm^{-1} with the N-C stretching modes. O-C-N bending vibration modes were also computed at 388 and 360 cm^{-1}. In the transition to the solvent environment there are about 1 cm^{-1} changes in the vibration frequencies. In these regions, there are very few shifts in the transition to solvent

environments. All calculated data are in agreement with the experimental ones.

Similar to bending modes, torsional modes are also predominantly calculated in low-wavenumbers regions. In this paper, the H-C-N-C torsional modes in the vacuum environment are predicted at 1113, 1110, 1045 and 813 cm^{-1}. O-N-C-C and O-N-N-C modes were calculated at 734, 729 and 689 cm^{-1} in vacuum. These vibrations were also observed in the experimental spectrum in accordance with the calculated values. While the presence of the solvent environments did not cause changes in the vibrational frequencies of some modes, it can cause severe changes in the vibrational frequencies of some modes.

3.3. The energetic and thermochemical properties of tbH

In Table 3, energies of tbH from DFT-PCM optimizations are presented in vacuum and solvent media. As seen from Table 3, with the increasing dielectric constant of media, energies of tbH in different solvent media have decreased. Thermochemical properties of tbH in different solvent media were also calculated and given in Table 3. The thermochemical analysis calculations were performed at 298.15 K temperature and 1.0 atm pressure. The calculated zero point vibrational energies of tbH in different media are 100.3394 Kcal/mol (vacuum Ɛ=1.00), 100.3248 Kcal/mol (DCM Ɛ=8.93), 100.2798 Kcal/mol (DMSO Ɛ=46.83) and 100.2731 Kcal/mol (water Ɛ=78.36). Increasing dielectric constants increase the dipole moment of tbH.

Table 3. The energies and thermochemical properties of tbH in 298.15 K calculated by DFT.

	Vacuum	Solvent Media		
		DCM	DMSO	H_2O
Tot. Energy (Hartree)	-641.247	-641.261	-641.263	-641.264
Zero-point vibr. Energy (kcal/mol)	100.339	100.325	100.280	100.273
$E_0=E_{tot}+ZPVE$ (Hartree)	-641.087	-641.101	-641.104	-641.104
$E_{298}=E_{el}+E_{vib}+E_{rot}+E_{trans}$ (Hartree)	-641.076	-641.090	-641.092	-641.092
$H_{298}=E_{298}+RT$ (Hartree)	-641.075	-641.089	-641.091	-641.091
$G_{298}=H_{298}-TS$ (Hartree)	-641.126	-641.139	-641.142	-641.142
Entropy (cal/mol.K)	108.332	106.739	106.901	106.969
Heat capacity (cal/mol.K)	41.881	41.812	41.823	41.826

In addition, some of the important thermal parameters such as entropy and heat capacity have increased as the dielectric constant of medium increases, but the values of these parameters were decreased in the solvent environment when compared to the gas phase.

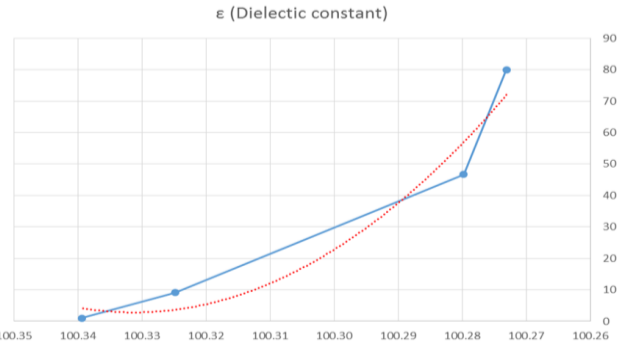

Figure 6. With increasing dielectric constant, energy exchanges of tbH.

3.4. Frontier molecular orbitals and chemical reactivity

In this work, we have also computed the highest occupied molecular orbital energies (HOMO), lowest unoccupied molecular orbital energies (LUMO) and their energy gaps for tbH. The gap between HOMO and LUMO energies is an important parameter in detection of molecular electrical transport (Breda *et al*. 2006, Shahidha *et al.* 2015) Moreover, the energy of the HOMO is directly related to the ionization potential, and LUMO energy is directly related to the electron affinity. This is used by the frontier electron density for estimating the most reactive position in p-electron systems and it is also explains several types of reaction in conjugated system (Shahidha *et al.* 2015).

Table 4. Calculated chemical reactivity (eV) and dipole moments of tbH in different media.

Parameters	Vacuum	DCM	DMSO	H_2O
E_{HOMO}	-6.454	-6.472	-6.474	-6.474
E_{LUMO}	-1.419	-1.399	-1.398	-1.397
$\Delta E_{LUMO-HOMO}$	5.035	5.073	5.076	5.077
electron affinity (A)	1.419	1.399	1.398	1.397
ionization potential (I)	6.454	6.472	6.474	6.474
global hardness (η)	2.5175	2.5365	2.5380	2.5385
chemical potential (μ)	-3.9365	-3.9355	-3.9360	-3.9355
electrophilicity (ω)	3.0777	3.0531	3.0520	3.0507
μ (Debye)	4.7479	6.1297	6.3663	6.3904

Table 4 shows the calculated electronic properties of tbH in different dielectric media. When Table 4 is examined, it is seen that HOMO energy increases and LUMO energy decreases with increasing dielectric constant of the environment.

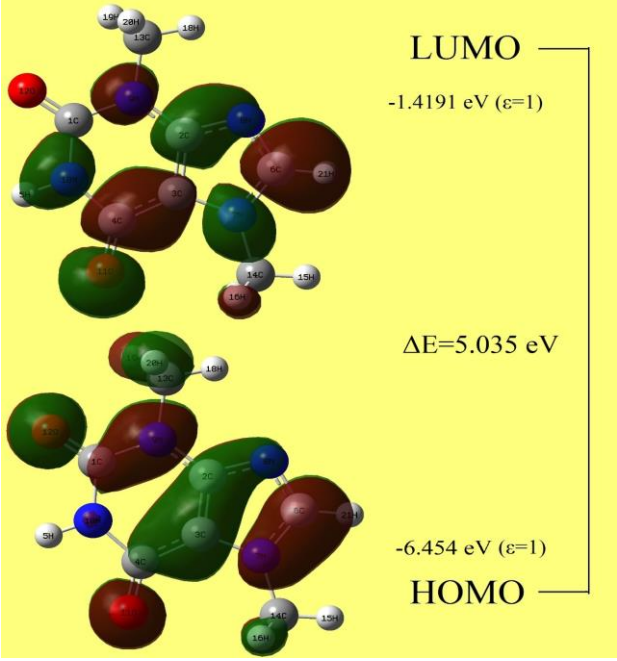

Figure 7. The HOMO-LUMO contour maps of tbH.

Figure 7 shows HOMO and LUMO contour maps of tbH in vacuum medium.

Considering Koopmans's theorem (Parr and Pearson 1983) ionization potential $I=-E_{HOMO}$ and electron affinity $A=-E_{LUMO}$ can be described. Parr et al. explained to chemical potential as $\mu=(E_{HOMO}+E_{LUMO})/2$, global hardness as $\eta=(E_{LUMO}-E_{HOMO})/2$ and finally electrophilicity as $\omega= \mu^2/2\eta$ (Brandl et al. 2001, Parr and Pearson 1983, Parr 1999).

3.5 Atomic charges

The net atomic charges of tbH atoms calculated by Mulliken Population Analysis (MPA) and Natural Population Analysis (NPA) are given in Table 5. Natural atomic charges are more reliable than those calculated by Mulliken (Breda *et al.* 2006). The charge distributions of tbH show that all nitrogen atoms are negative while the hydrogen atoms are positive. In addition, the atomic charges of oxygen atoms are rich in negative charges. For the 2C atom, the Mulliken atomic charge is negative, but the natural charge is positive. In addition, the solvent medium significantly affects the atomic charge of tbH.

Table 5. The Mulliken and Natural atomic charges (in e) of tbH.

Atom	Vacuum		DCM		DMSO		H_2O	
	Mlkn Chrg	Ntrl Chrg	Mlkn Chrg	Ntrl Chrg	Mlkn Chrg	Ntrl Chrg	Mlkn Chrg	Ntrl Chrg
1C	0.36	0.82	0.39	0.83	0.40	0.83	0.40	0.83
2N	-0.17	-0.48	-0.15	-0.47	-0.15	-0.46	-0.15	-0.46
3C	-0.09	0.38	-0.06	0.39	-0.05	0.39	-0.05	0.39
4C	-0.05	-0.03	-0.04	-0.03	0.04	-0.03	0.04	-0.03
5C	-0.07	-0.64	-0.05	-0.64	-0.05	-0.65	-0.05	-0.65
6N	-0.43	-0.64	-0.42	-0.63	-0.42	-0.63	-0.42	-0.63
7O	-0.34	-0.63	-0.42	-0.67	-0.43	-0.68	-0.43	-0.68
8H	0.39	0.42	0.40	0.43	0.40	0.43	0.40	0.43
9C	-0.27	-0.36	-0.29	-0.36	-0.29	-0.36	-0.29	-0.36
10H	0.18	0.22	0.18	0.22	0.18	0.22	0.18	0.22
11H	0.19	0.22	0.20	0.21	0.20	0.21	0.20	0.21
12H	0.20	0.20	0.20	0.21	0.20	0.21	0.20	0.21
13N	-0.20	-0.53	-0.27	-0.55	-0.28	-0.55	-0.28	-0.55
14C	0.24	0.26	0.25	0.28	0.25	0.28	0.25	0.28
15N	-0.13	-0.37	-0.11	-0.36	-0.10	-0.36	-0.10	-0.36
16O	-0.34	-0.62	-0.40	-0.66	-0.42	-0.66	-0.42	-0.66
17C	-0.30	-0.35	-0.31	-0.35	-0.31	-0.35	-0.31	-0.35
18H	0.13	0.20	0.15	0.22	0.16	0.22	0.16	0.22
19H	0.21	0.22	0.20	0.22	0.21	0.22	0.21	0.22
20H	0.21	0.22	0.20	0.22	0.21	0.22	0.21	0.22
21H	0.22	0.20	0.25	0.21	0.26	0.21	0.26	0.22

3.6. tbH-H_2O complexes

As we mentioned in the introduction of this paper, the most basic situation in the investigation of solvent effects on biological molecules is to consider water complexes. Hydrogen bonded complexes form between a hydrogen atom attached to an electronegative donor atom and a neighboring acceptor atom. Here, hydrogen bonded tbH-H_2O complexes were studied using the DFT/B3LYP method. Since the tbH molecule has N and O heteroatoms and therefore lone pair (lp) electrons, it can form intermolecular H-bonds of the type lpN···H–O and lpO···H–O with H_2O molecules. The tbH-H_2O complexes investigated in this study were studied for the presence of a maximum of eight water molecules adjacent to tbH in the presence of hydrogen bonding. Nine versions have been proposed for one-two H_2O bonding states, and for these versions, energies and hydrogen bond lengths have been investigated.

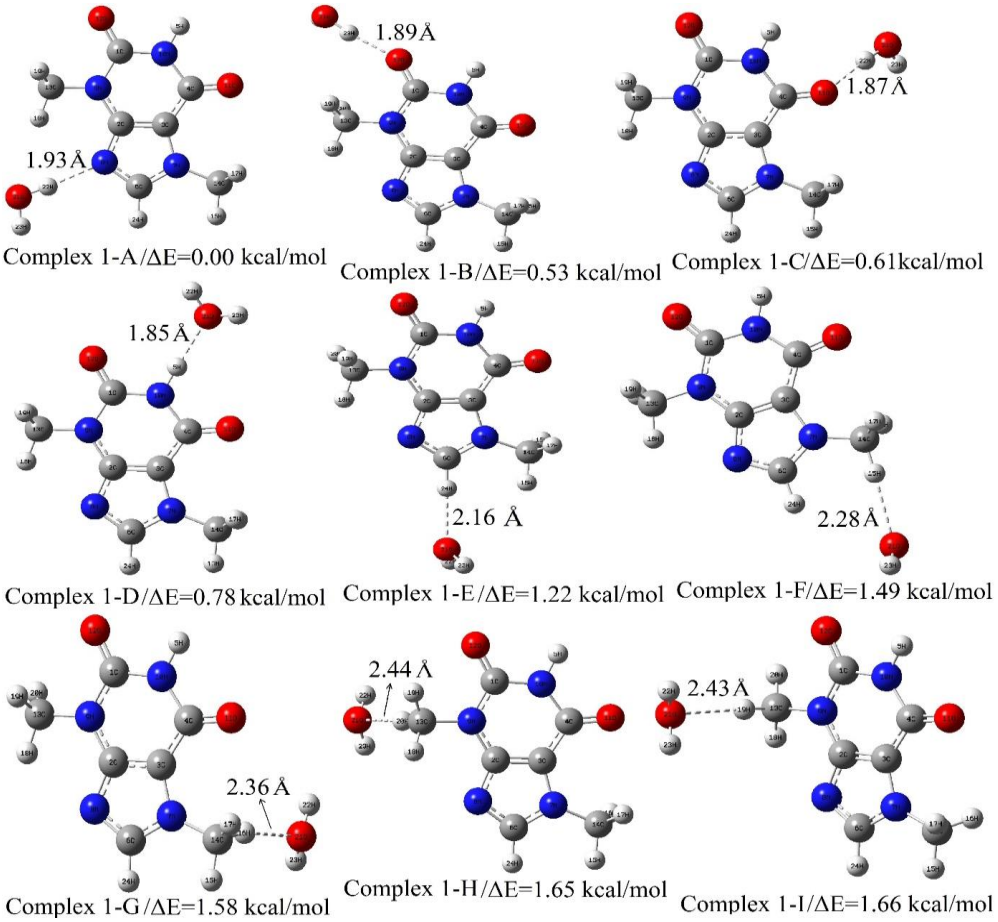

Figure 8. The optimized structures of 1-1 bonded tbH-H_2O complexes

Figure 8 shows that the most stable structure of 1-1 bonded tbH-H_2O complexes is the 1-A complex. This structure has an lpN···H–O type intermolecular H-bond and length of this bond was calculated to be 1.93 Å. When examined in terms of energy, the lowest energetic versions of the 1-1 tbH complexes are those hydrogens bonded ones in the form of lpN···H-O and lpO···H–O. It is known that hydrogen bonds of these types are strong. On the other hand, the common point of these three versions is that hydrogen atoms of water molecules are bonded to oxygen and nitrogen atoms of tbH but in other versions, hydrogen bonds are formed between oxygen atoms of water molecule and hydrogen atoms of tbH. Therefore, for the other versions it can be said that bond strength is weaker and bond lengths are taller. 1-2 bonded tbH-H_2O complexes are seen in Figure 9. The most striking property of these complexes is that the structures with hydrogen bonds of the form lpN···H-O and lpO···H-O are the most stable structures. In all structures, approximate O-H···O distances are 1.88-1.89 Å and O-H···N distance is 1.94 Å. In the C-H···O hydrogen bonds, distances vary between 2.16-2.48 Å.

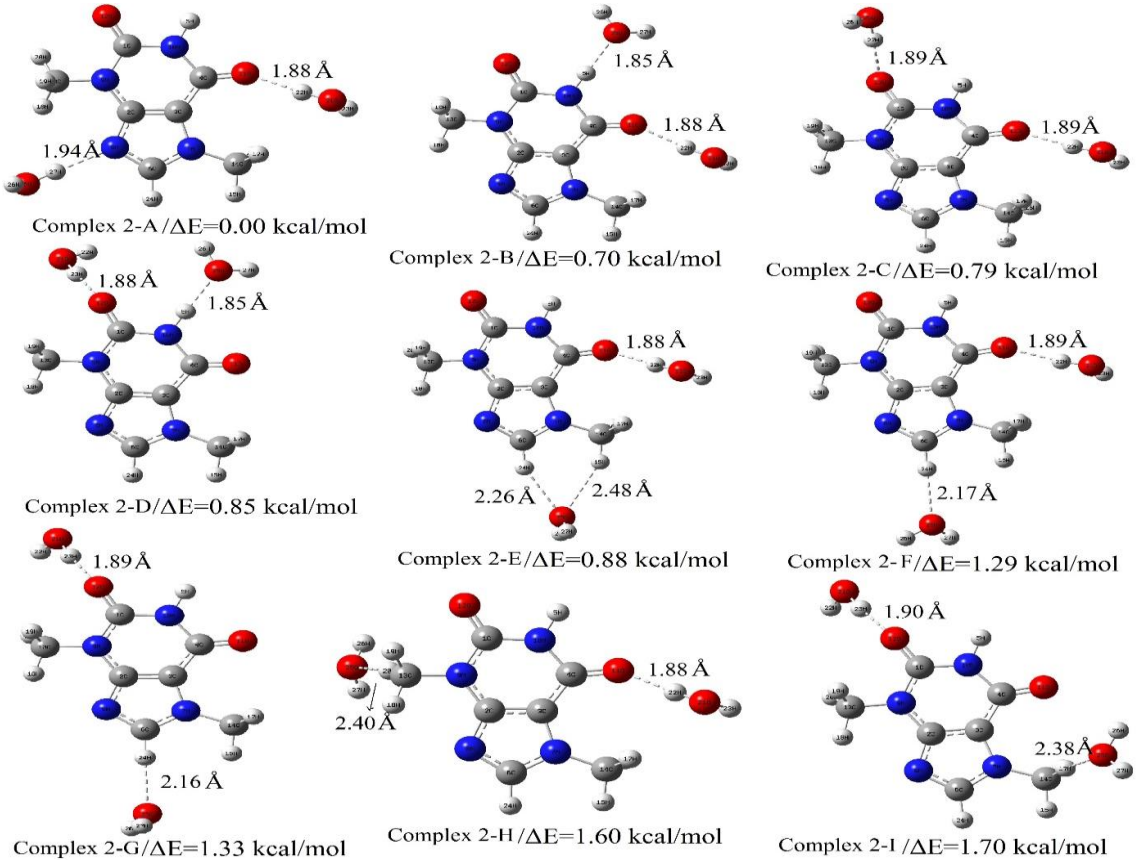

Figure 9. The optimized structures of 1-2 bonded tbH-H2O complexes.

Table 6. Total energies (au) and relative energies (kcal/mol) of tbH-1H_2O, tbH-2H_2O and tbH-3H_2O complexes.

Strc.	1-1 Comp.	Δ	1-2 Comp.	Δ	1-3 Comp.	Δ
V1	-717.74718	0.00	-794.22156	0.00	-870.69601	0.00
V2	-717.74633	0.53	-794.22044	0.70	-870.69599	0.02
V3	-717.74621	0.61	-794.22030	0.79	-870.69555	0.29
V4	-717.74594	0.78	-794.22020	0.85	-870.69532	0.44
V5	-717.74523	1.22	-794.22016	0.88	-870.69463	0.87
V6	-717.74481	1.49	-794.21950	1.29	-870.69452	0.94
V7	-717.74466	1.58	-794.21943	1.33	-870.69428	1.09
V8	-717.74454	1.65	-794.21901	1.60	-870.69348	1.59
V9	-717.74453	1.66	-794.21885	1.70		

Figure 10 shows 1-3 bonded eight different versions of tbH-H_2O complexes. As shown in the Figure, the most stable structure among these eight structures is the one with lpN···H-O and lpO···H-O connections similar to 1-1 and 1-2. Unlike the others, it can be seen from Table 6 that the energy difference between V1 and V2 is very small. Calculated energy difference is only 0.02 kcal/mol. Therefore, from the results of the theoretical calculations, it cannot be clearly determined, which 1-3 connections are favorable?

Table 7. Total energies (au) and relative energies (kcal/mol) of tbH-4H_2O, tbH-5H_2O, tbH-6H_2O, tbH-7H_2O and tbH-8H_2O complexes. ($\Delta=|EV_1-EV_X|$)

Structure	V1	V2	V3	V4
1-4 Complex	-947.17031	-947.16912	-947.16790	-947.16755
Δ	0.00	0.74	1.51	1.73
1-5 Complex	-1023.64276	-1023.64262	-1023.64221	-1023.64209
Δ	0.00	0.09	0.34	0.42
1-6 Complex	-1100.12024	-	-	-
1-7 Complex	-1176.58970	-	-	-
1-8 Complex	-1253.06677	-	-	-

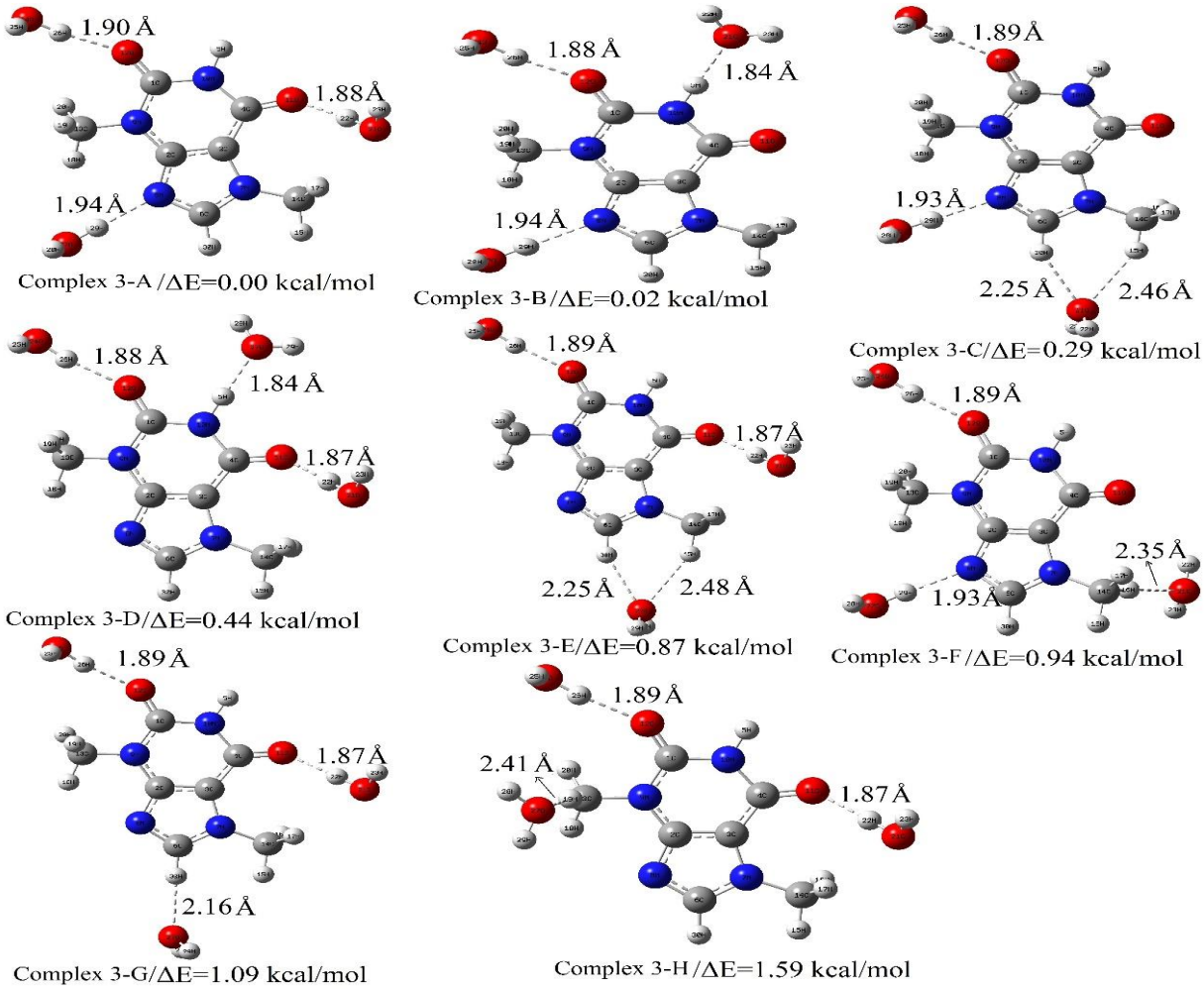

Figure 10. The optimized structures of 1-3 bonded tbH-H_2O complexes.

In Figure 11, possible 1-4, 1-5, 1-6, 1-7 and 1-8 bound tbH-H_2O complexes are plotted and the calculated energies and energy differences were given in Table 7. Four different combinations have been proposed for 1-4 bonded complexes. When the most stable versions of these structures are investigated, it is seen that the N···H-O and O···H-O type hydrogen bonded structures are most stable. Total energy of version 4A is 0.74 kcal/mol lower than complex 4B. The only difference between Complex 4B and Complex 4C is that only one of the 4 water molecules bonded to the tbH is bound by hydrogen bonds from two points. This causes a difference of about 0.77 kcal/mol in the energy and therefore a more stable structure. Figure 11 also shows 1-5 bonded tbH-H_2O complexes. It is seen that the calculated energy values for 1-5 bonded complexes are very close to each other. Only one version of 1-6, 1-7, and 1-8 complexes were studied. Especially after the addition of the eighth water molecule, it was seen that the optimizations ended when the water molecules were clustered. In 1-6 bonded complex, total energy was calculated as -1100.12024 Hartree. H-bond lengths vary between 1.82-1.88 Å for O···H-O, 1.95 Å for N···H-O and 2.40 Å for O···H-C. For the tbH-7H_2 complex, total energy was calculated as -1176.58970 Hartree. H-bond lengths vary between 1.84-2.42 Å.

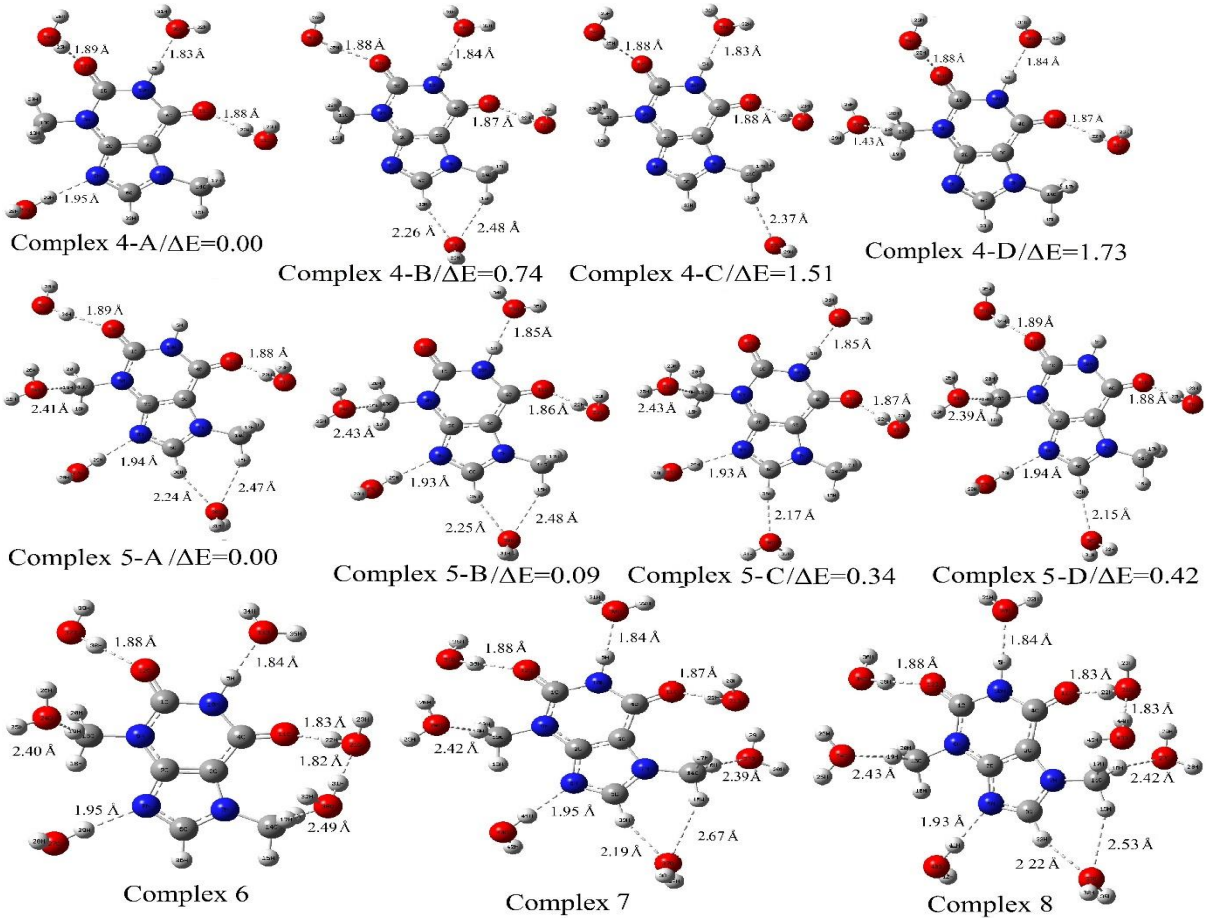

Figure 11. The optimized structures of 1-4, 1-5, 1-6, 1-7 and 1-8 bonded tbH-H_2O complexes.

4. Conclusions

In this paper, we have investigated to the solvent effects on structural, spectroscopic, electronic and thermochemical properties of tbH. The investigations were carried out in DCM, DMSO, H_2O and vacuum environments. From this study, it can be said that the stable equilibrium energy has reduced in solvent media depending on the dielectric constant. tbH is more stable in the solvent environments. The geometric parameters calculated in non-polar solvent environment and polar solvent environment are different from each other. This case shows that polarity difference of solvents leads to the formation of different geometric structures. For the tbH molecule, vibrational frequencies and their intensities were affected significantly from solvent environments but in the solvents of same polarity shifts were observed minor. While the frontier orbitals of tbH are virtually unaffected by the solvent medium, the atomic charges have affected importantly. It is seen from the results of this study that N···H-O and O···H-O hydrogen bonded structures are more stable than others are. Calculated hydrogen bond lengths for all tbH-H_2O complexes are range from 1.8-2.5 Å.

References

Bernal-Uruchurtu, M. I., Kerenskaya, G., Janda, K. C., 2009, *International Reviews in Physical Chemistry*, **28**, 223-265.

Bilkan, M. T., 2017. Structural and spectroscopic studies on dimerization and solvent-ligand complexes of Theobromine. *Journal of Molecular Liquids*, **238**, 523-532.

Brandl, M., Meyer, M., Sühnel, J. J., 2001. Quantum-Chemical Analysis of C-H…O and C-H…N Interactions in RNA Base Pairs—H-Bond Versus Anti-H-Bond Pattern. *Journal of biomolecular Structure & Dynamics*, **18**, 4, 545-555.

Breda, S., Reva, I.D., Lapinski, L., Nowak, M.J., Fausto, R., 2006. Infrared spectra of pyrazine, pyrimidine and

pyridazine in solid argon. *Journal of Molecular Structures*, **786**, 193-206.

Calabrese, C., Gou, Q., Spada, L., Maris, A., Caminati, W., Melandri, S. 2016. Effects of Fluorine Substitution on the Microsolvation of Aromatic Azines: The Microwave Spectrum of 3-Fluoropyridine-Water. *Journal of Physical Chemistry A*, **120**, 27, 5163-5168.

Cook, D., Regnier, Z. R., 1967. The infrared spectra of theobromine salts. *Canadian Journal of Chemistry*, **45**, 2899-2902.

Dennington, R. D., Keith, T. A., Millam, J. M. GaussView 5, Gaussian, Inc, 2008.

Ford, K. A., Ebusuzaki, Y., Boyle, P. D., 1998. Methylxanthines. II. Anhydrous Theobromine. *Acta Crystallographica*, **C54**, 1980-1983.

Fornaro, T., Burini, D., Biczysko, M., Barone, V. 2015. Hydrogen-Bonding Effects on Infrared Spectra from Anharmonic Computations: Uracil–Water Complexes and Uracil Dimers. *Journal of Physical Chemistry A*, **119**, 4224-4236.

Frisch, M.J., Trucks, G.W., Schlegel, H.B., Scuseria, G.E., Robb, M.A., Cheeseman, J.R., Montgomery Jr., J.A., Vreven, T., Kudin, K.N., Burant, J.C., et al. 2003, Gaussian 03, revision D.01, Gaussian Inc., Wallingford, CT.

Jamróz, M.H., 2004, "Vibrational Energy Distribution Analysis" VEDA 4, Warsaw.

Kwak, K., Rosenfeld, D. E., Chung, J. K., Fayer, M. D, 2008. Solute−Solvent Complex Switching Dynamics of Chloroform between Acetone and Dimethylsulfoxide−Two-Dimensional IR Chemical Exchange Spectroscopy. *Journal of Physical Chemistry B*, **112**, 13906-13915.

Miertuš, S., Scrocco, E., Tomasi, 1981. Electrostatic interaction of a solute with a continuum. A direct utilizaion of AB initio molecular potentials for the prevision of solvent effects. *Journal of Chemical Physics*, **55**, 117-129.

Mikulski, C. M., Grossman, S., Lee, C. J., 2007. Hypoxanthine, xanthine and theobromine complexes with palladium(II) and platinum(IV) chlorides. *Transition Metal Chemistry*, **12**, 21-25.

Mourik, T. V., Price, S. L., Clary, D. C., 1999. Ab Initio Calculations on Uracil−Water. *Journal of Physical Chemistry A*, **103**, 1611-1618.

Oettl, K., Reibnegger, G., 1999. Pteridines as inhibitors of xanthine oxidase: structural requirements. *Biochimica Biophysica Acta*, **1430**, 387.

Parr, R.G., Pearson, R.G., 1983. Absolute hardness: companion parameter to absolute electronegativity. *Journal of American Chemical Society*, **105**, 7512-7516.

Parr, R.G., 1999. Electrophilicity Index. *Journal of American Chemical Society*, **121**, 1922-1924.

Parthasarathi, R., Subramanian, V., Sathyamurthy, N., 2005. Hydrogen Bonding in Phenol, Water, and Phenol−Water Clusters. *Journal of Physical Chemistry A*, **109**, 843-850.

Shahidha, R., Al-Saadi, A. A., Muthu, S., 2015. Vibrational spectroscopic studies, normal co-ordinate analysis, first order hyperpolarizability, HOMO–LUMO of midodrine by using density functional methods. *Spectrochimica Acta Part A*, **134**, 127-142.

Tewari, B. B., Beaulieu-Houle, G., Larsen, A., Kengne-Momo, R., Auclair, K., Butler, I. S. 2012. An Overview of Molecular Spectroscopic Studies on Theobromine and Related Alkaloids. *Applied Spectroscopy Review*, **47**, 163-179.

Ucun, F., Sağlam, A., Güçlü, V., 2007. Molecular structures and vibrational frequencies of xanthine and its methyl derivatives (caffeine and theobromine) by ab initio Hartree–Fock and density functional theory calculations. *Spectrochimica Acta A*, **67**, 342-349.

Wang, Y., Liu, Q., Qui, L., Wang, T., Yuan, T., Lin, J., Luo, S., 2015. Molecular structure, IR spectra, and chemical reactivity of cisplatin and transplatin: DFT studies, basis set effect and solvent effect. *Spectrochimica Acta A*, **150**, 902-908.

Yurdakul, Ş. Bilkan, M., T., 2015. Spectroscopic and structural properties of 2, 2′-dipyridylamine and its palladium and platinum complexes. *Optics and Spectroscopy*, **119**, 4, 603-619.